THEORETICA CHIMICA ACTA
Theoret. Chim. Acta (Berl.) 65, 303–310 (1984)

Momentum density and molecular geometry. Bent BH_2^- and linear BH_2^+

Toshikatsu Koga*

Department of Applied Chemistry and Department of Applied Science for Energy, Muroran Institute of Technology, Muroran, Hokkaido, 050 Japan

Hisayoshi Kobayashi

Faculty of Living Science, Kyoto Prefectural University, Kyoto, 606 Japan

Based on a special form of the molecular virial theorem, the recently proposed method of momentum density for interatomic interactions is here applied to the problem of molecular geometry. Two molecules BH_2^- and BH_2^+, which have the same nuclear framework but favor respectively bent and linear conformations, are comparatively studied. Using an approximate Hartree–Fock momentum density, the total molecular energy (including the nuclear repulsion) is partitioned into orbital components, and a geometry correlation diagram is derived. An atom-bond partitioning of the total energy is also examined based on the one- and two-center decomposition of the momentum density.

Key words: Momentum density—BH_2^- and BH_2^+—geometries of ~—virial theorem

1. Introduction

In previous papers, we have proposed [1] and developed [2–4] a method of momentum density which enables us to clarify the momentum-space origin of nuclear rearrangements such as molecular geometries and chemical reactions. Rigorous relations between the momentum density and the molecular total energy have been derived [1–4], and the importance of the concept of contraction (i.e.

* To whom all correspondence should be addressed.

an increase of low-momentum density with a simultaneous decrease of high-momentum density, and expansion (i.e. a reorganization of the momentum density reverse to the contraction) has been suggested [1]. The method has been applied to several diatomic interactions [5–8] and the applicability of the method has been recently discussed in some detail [4].

The purpose of this study is to apply the proposed method of momentum density to the bending process of triatomic molecules, and to investigate the bent-linear geometry correlation in these systems from the momentum space viewpoint. We have chosen BH_2^- and BH_2^+ molecules for this purpose, because these molecules consist of the same nuclei but favor different molecular geometries (i.e. bent and linear) depending on the number of electrons (i.e. 8 and 6 electrons). An outline of the momentum density approach employed here is given in the next section together with the computational details. The results for BH_2^- and BH_2^+ are discussed and compared with each other in Sect. 3. Atomic units are used throughout this paper.

2. Theoretical ground

Nelander showed [9–11] that the polyatomic virial theorem can be written as

$$T(\boldsymbol{R}, \boldsymbol{\Theta}) + E(\boldsymbol{R}, \boldsymbol{\Theta}) + \sum_{i=1}^{n} R_i[\partial E(\boldsymbol{R}, \boldsymbol{\Theta})/\partial R_i] = 0. \tag{1}$$

$\{\boldsymbol{R}, \boldsymbol{\Theta}\}$ are the minimal set of internal coordinates consisting of n bond lengths $\boldsymbol{R} = \{R_1, R_2, \ldots, R_n\}$ and m bond angles $\boldsymbol{\Theta} = \{\theta_1, \theta_2, \ldots, \theta_m\}$ which are sufficient to specify the conformation of a given molecular system. $T(\boldsymbol{R}, \boldsymbol{\Theta})$ and $E(\boldsymbol{R}, \boldsymbol{\Theta})$ denote the kinetic and total energies of the system, respectively. Under the optimum condition of the all bond lengths involved, $\partial E/\partial R_i = 0$ $(i = 1, 2, \ldots, n)$, the virial theorem (1) takes a simple atom-like form $E(\boldsymbol{R}_{\text{opt}}, \boldsymbol{\Theta}) = -T(\boldsymbol{R}_{\text{opt}}, \boldsymbol{\Theta})$ even for a non-equilibrium conformation of the molecular system. Since the kinetic energy T is just half the second moment $\langle |\boldsymbol{p}|^2 \rangle$ of the momentum density $\rho(\boldsymbol{p})$, the total energy E of a molecular system, including the nuclear repulsion energy, is completely determined by the momentum density $\rho(\boldsymbol{p})$ [4]. That is,

$$E(\boldsymbol{\Theta}) = -T(\boldsymbol{\Theta}) = -\int \mathrm{d}\boldsymbol{p}\, (|\boldsymbol{p}|^2/2)\rho(\boldsymbol{p}; \boldsymbol{\Theta}), \tag{2}$$

where the parameter $\boldsymbol{R}_{\text{opt}}$ has been omitted for the sake of simplicity. The momentum density $\rho(\boldsymbol{p})$ is defined by $\rho(\boldsymbol{p}) \equiv N \int d\boldsymbol{p}_2 \cdots d\boldsymbol{p}_N |\Phi(\boldsymbol{p}, \boldsymbol{p}_2, \ldots, \boldsymbol{p}_N)|^2$ with N being the number of electrons, and the momentum wave function $\Phi(\boldsymbol{p}_1, \ldots, \boldsymbol{p}_N)$ is obtained from the ordinary position wave function $\Psi(\boldsymbol{r}_1, \ldots, \boldsymbol{r}_N)$ by the Dirac–Fourier transformation

$$\Phi(\boldsymbol{p}_1, \ldots, \boldsymbol{p}_N) = (2\pi)^{-3N/2} \int d\boldsymbol{r}_1 \cdots d\boldsymbol{r}_N \exp\left(-i \sum_{j=1}^{N} \boldsymbol{p}_j \boldsymbol{r}_j\right) \Psi(\boldsymbol{r}_1, \ldots, \boldsymbol{r}_N).$$

Since the kinetic energy operator $|\boldsymbol{p}|^2/2$ appearing in Eq. (2) is angular-independent, Eq. (2) is simplified to [4]

$$E(\Theta) = -T(\Theta) = -\int_0^\infty dp\,(p^2/2) I(p;\Theta), \tag{3}$$

where $p = |\boldsymbol{p}|$ and $I(p;\Theta) \equiv p^2 \int_0^{2\pi} d\phi_p \int_0^\pi d\theta_p \sin\theta_p \rho(\boldsymbol{p};\Theta)$ is the radial momentum density. Eq. (3) constitutes the basic equation of the present study, and in Ref. [4] this approach has been referred to as Method (B).

It is then clear from Eq. (3) that a partitioning of the radial momentum density $I(p;\Theta)$ into some components results in the corresponding partitioning of the total energy $E(\Theta)$. The following two partitionings are examined here.

(a) Orbital partitioning: Within the framework of independent-particle models, the (radial) momentum density is given as the sum of orbital contributions. As a result, the total energy is expressed as an exact sum of orbital components. Takahata and Parr [12] stressed that no other additive decompositions of the total energy are known at the Hartree–Fock level of accuracy, and gave a plot of the orbital kinetic energy for H_2O molecule based on the first equality of Eq. (3).

(b) Atom-bond partitioning: For LCAO wave functions, the (radial) momentum density can be separated into the contributions from atoms and bonds according to the centers of constituent AO's. The total energy is then given as the sum of these components, though this partitioning is basis-dependent similar to the Mulliken population analysis.

For BH_2^- and BH_2^+ molecules, we have assumed the C_{2v} geometries which are specified by a set of two internal coordinates R(B—H bond length) and θ (HBH bond angle). For both molecules, approximate Hartree–Fock wave functions have been calculated as a function of θ using the GAUSSIAN80 program package [13] with the 6-31G** basis. At every θ, the optimizations of the orbital exponents and the bond length R have been carried out simultaneously, which guarantee the validity of Eq. (3). The exponent optimization has been performed by introducing a single scaling factor common to all the orbital exponents.

3. Results and discussion

We discuss the bending processes of BH_2^- and BH_2^+ molecules using the results of linear conformations as references. As θ decreases from 180°, BH_2^- molecule becomes stable and the equilibrium conformation is calculated to be $\theta = 97.80°$ and $R = 2.413$ with $E = -T = -25.674$. On the other hand, BH_2^+ molecule becomes unstable with the decrease of θ, and the molecule is most stable at the linear shape ($R = 2.203$) with $E = -T = -25.473$.

In Fig. 1, the reorganization of the radial momentum density ΔI from the linear conformation is shown for the two molecules. The change in the kinetic energy density $(p^2/2)\Delta I$ is also given which represents the contribution of the momentum density to the kinetic energy. (Hereafter, the symbol Δ is used to denote the net

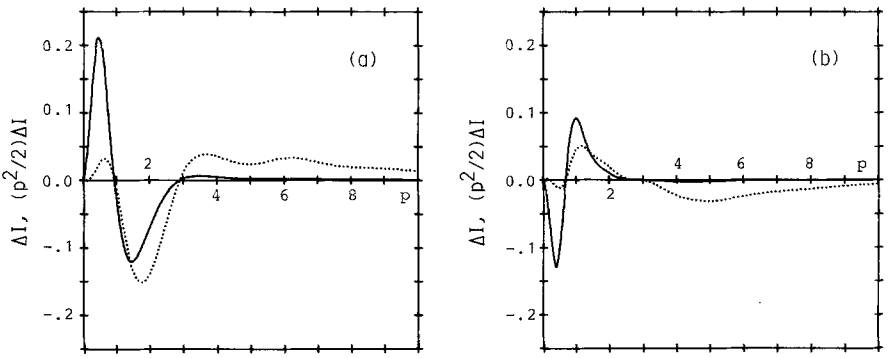

Fig. 1. Reorganizations of the radial momentum density $\Delta I(p)$ (solid line) and the kinetic energy density $(p^2/2)\Delta I(p)$ (dotted line) from the linear conformation. (a) BH_2^- molecule at $\theta = 97.80°$. (b) BH_2^+ molecule at $\theta = 90°$

change from $\theta = 180°$.) For BH_2^- molecule (Fig. 1a, $\theta = 97.80°$), ΔI shows both the contractive and expansive reorganizations. The contraction in the low momentum region is mainly due to the valence orbitals, while the expansion in the high momentum region is mainly due to the boron $1s$ core orbital (see Sect. 3.1). As the curve for $(p^2/2)\Delta I$ shows, the latter gives a larger energetic contribution, and the total reorganization is expansion which corresponds to the positive ΔT and hence the stabilization of the system by $\Delta E = -0.067$. For BH_2^+ molecule (Fig. 1b, $\theta = 90°$), the situation is approximately opposite and the total reorganization is contraction. This is the momentum density origin of the destabilization ($\Delta E = 0.119$) of this system. We further examine these opposite changes in BH_2^- and BH_2^+ molecules in terms of the two partitioning methods mentioned in Sect. 2.

3.1. Orbital partitioning

Using the orbital kinetic energy Δt_i, we show the orbital partitioning of the total energy in Fig. 2 as a function of the bond angle θ. The corresponding momentum density origin is given in Fig. 3 for $\theta = 97.80°(BH_2^-)$ and $\theta = 90°(BH_2^+)$.

In Fig. 2, it is seen that all the orbitals can be classified according to their roles in the bent-linear correlation. Common to the both molecules, the $3a_1$ orbital gives bending contribution, whereas the $2a_1$ and $2b_2$ orbitals give linearizing contribution. The $1b_1$ orbital is almost indifferent. The contribution of the $1a_1$ orbital is rather small and shows a trend similar to the total sum. The exponent optimization by a single factor is considered for the $1a_1$ contribution, since this procedure may induce the same change that the whole molecule favors to the core ($1a_1$) orbital. However, the $1b_2$ and $4a_1$ orbitals play different roles in the two molecules. In BH_2^- molecule, the $3a_1$ (HOMO) gives the largest bending contribution and this orbital seems essential for the bent equilibrium conformation. In BH_2^+ molecule, however, the $1b_2$ orbital (HOMO) is almost indifferent, and the $2a_1$ orbital (next HOMO) gives a predominant contribution to the total curve. In the present analysis, the highest a_1 orbitals seem important to determine

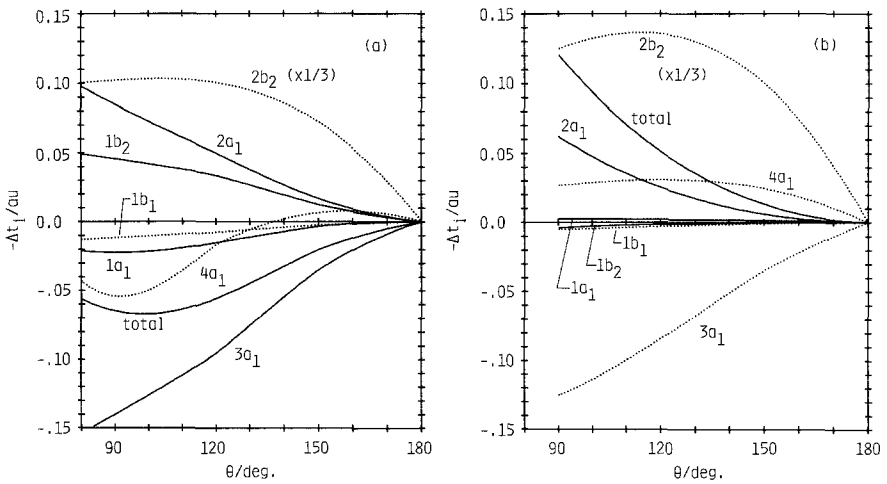

Fig. 2. Orbital partitioning of the negative kinetic energy. The orbital contribution refers to single electron, while the total contribution refers to all electrons. Solid and dotted lines mean occupied and virtual orbitals, respectively. (a) BH_2^- molecule. (b) BH_2^+ molecule

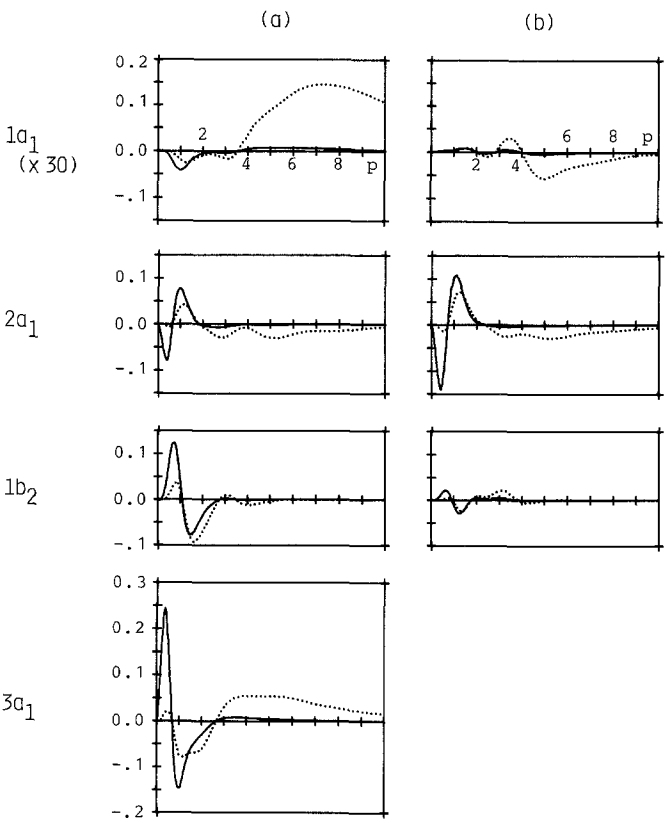

Fig. 3. Orbital partitioning of the reorganizations $\Delta I(p)$ (solid line) and $(p^2/2)\Delta I(p)$ (dotted line). (a) BH_2^- molecule at $\theta = 97.80°$. (b) BH_2^+ molecule at $\theta = 90°$

the shapes of the molecule. The order of the magnitude of orbital contributions is approximately $1b_1$ (indifferent) $< 1a_1$ (bent or indifferent) $\lesssim 1b_2$ (linear or indifferent) $\lesssim 4a_1$ (bent or linear) $< 2a_1$ (linear) $< 3a_1$ (bent) $< 2b_2$ (linear).

The above results do not agree with the well-known Walsh rule [14] (for other models for molecular geometry, see e.g. [15]) except for the $3a_1$ and $1b_1$ orbitals, though the present bent-linear classification of the orbital contribution is based on an exact partitioning scheme. The corrected Walsh rule for AH_2-type molecule is known to be $2a_1$ (bent), $1b_2$ (linear), $3a_1$ (bent), and $1b_1$ (indifferent) in the increassing order of the orbital energy. Although the Walsh model includes the undefined concept of orbital binding energies, the role of the nuclear repulsion (which is not explicit in the Walsh model) seems to be essential for the above discrepancy. A more extensive study on the variety of molecules is needed to clarify this point.

On the basis of ΔI and $(p^2/2)\Delta I$ for individual orbitals given in Fig. 3, we can understand the correspondence between the contraction/expansion of the orbital momentum density and the negative/positive contribution of the orbital kinetic energy. When compared with the $1b_2$ orbital where only the valence AO's participate, the a_1 orbitals are characterized by small but long tails in the high momentum region due to the contribution of the boron $1s$ AO. The reorganization of the $1a_1$ orbitals are very small and show expansion (BH_2^-) and contraction (BH_2^+). The $1b_2$ orbitals are contractive (BH_2^-) and slightly expansive (BH_2^+). The $2a_1$ and $3a_1$ orbitals include both patterns of the contractive and expansive reorganizations. Since the reorganization in the high momentum region is significant energetically, the $2a_1$ orbital is contractive and the $3a_1$ orbital is expansive.

3.2. *Atom-bond partitioning*

In Fig. 4, the total energy is partitioned into the contributions from the atoms B and 2H and the bonds 2(B—H) and H—H for the bending processes of BH_2^- and BH_2^+ molecules. For both cases, the 2H contribution is bending, the B and 2(B—H) contributions are linearizing, and the H—H contribution is almost zero.

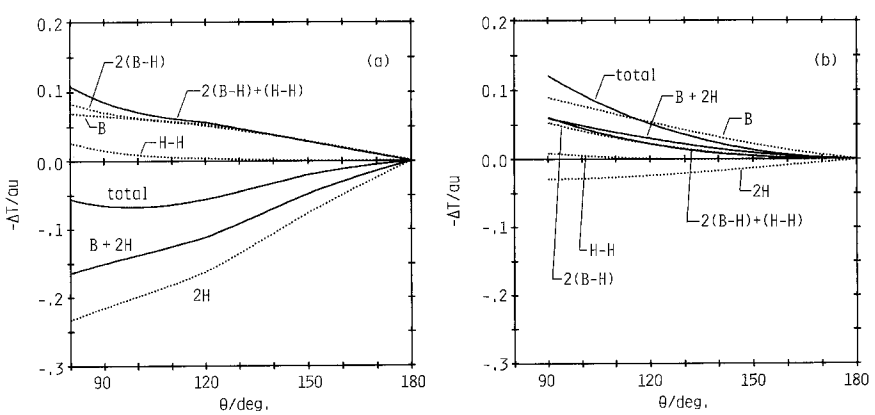

Fig. 4. Atom-bond partitioning of the negative kinetic energy. (a) BH_2^- molecule. (b) BH_2^+ molecule

The atomic contribution B+2H is larger than the bond contribution 2(B—H)+(H—H). Then the relative magnitudes of the linearizing B component and the bending 2H component determine the stable conformations of the molecules. The bending 2H is dominant in BH_2^- molecule, whereas the linearizing B is dominant in BH_2^+ molecule. These observations are related to the change in the electron population of each component.

The momentum density origin of the atom-bond partitioning is shown in Fig. 5. For the atom and bond components of the momentum density, the normalization relation does not hold, and therefore the concept of contraction and expansion does not apply to the atom-bond partitioning. Alternatively, the integration of a component ΔI over $[0, \infty)$ yields the change of the Mulliken population of the corresponding component. Generally, an increase (a decrease) of the population of some part raises (lowers) the kinetic pressure leading to an increase (a decrease) of the kinetic energy of that part. In the case of BH_2^-, the population flows mainly from the 2(B—H) to the 2H part with the decrease of θ, and this is the origin of the large bending contribution of the 2H part. In BH_2^+ molecule, the population

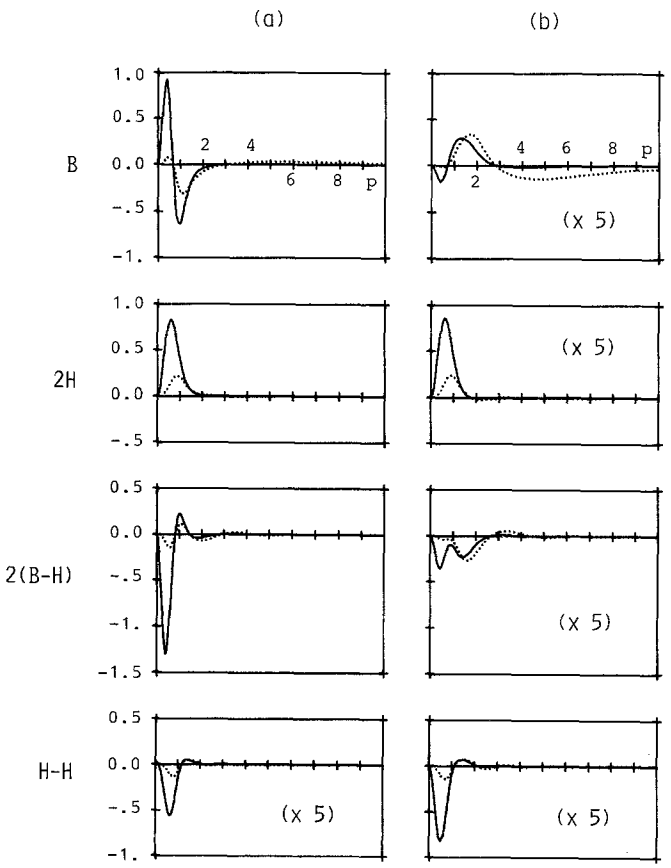

Fig. 5. Atom-bond partitioning of the reorganizations $\Delta I(p)$ (solid line) and $(p^2/2)\Delta I(p)$ (dotted line). (a) BH_2^- molecule at $\theta = 97.80°$. (b) BH_2^+ molecule at $\theta = 90°$

flows from the 2(B—H) and H—H parts to the B and 2H parts. Then, the 2H part contributions to bending. However, in the B part, the valence population predominantly increases accompanying a slight decrease of the $1s$ population. The momentum density then increases around $p \sim 1.3$ and decreases for $p > 2.8$. This lowering of the high-momentum density causes the linearizing contribution of the B part in BH_2^+ molecule.

4. Summary

Using the momentum density and the resultant kinetic energy, the bending processes of BH_2^- and BH_2^+ molecules have been comparatively studied. Though the molecules favor different conformations, some common features have been clarified. In the orbital partitioning, each orbital has been classified whether it contributes to bending or linearizing. The results have been common to the two molecules except for the $1a_1$, $1b_2$, and $4a_1$ orbitals, and a systematic investigation of the orbital kinetic energy is suggested as a possible exact decomposition of the total energy. The highest a_1 orbitals, $3a_1$ for BH_2^- and $2a_1$ for BH_2^+, have been found to be important to determine the stable geometry. In the atom-bond partitioning, the atomic components have been dominant. The contribution of the central B atom is linearizing, while that of the terminal H atoms is bending. The bent BH_2^- and linear BH_2^+ geometries are understood as the result of the relative dominance of these opposing contributions.

Acknowledgments. The Data Processing Center of Kyoto University is acknowledged for generous use of the FACOM M382/380 computer. Part of this study has been supported by a Grant-in-Aid for Scientific Research from the Ministry of Education of Japan.

References

1. Koga, T.: Theoret. Chim. Acta (Berl.) **58**, 173 (1981)
2. Koga, T., Morita, M.: Theoret. Chim. Acta (Berl.) **59**, 639 (1981)
3. Koga, T., Miyahara, T., Morita, M.: Theoret. Chim. Acta (Berl.) **63**, 377 (1983)
4. Koga, T., Morita, M.: Theoret. Chim. Acta (Berl.) **61**, 73 (1982)
5. Koga, T., Morita, M.: Theoret. Chim. Acta (Berl.) **59**, 423 (1981)
6. Koga, T., Sugawara, M., Morita, M.: Theoret. Chim. Acta (Berl.) **61**, 87 (1982)
7. Koga, T., Shimokawa, K., Inagawa, I., Morita, M.: Theoret. Chim. Acta (Berl.) **62**, 39 (1982)
8. Koga, T.: Int. J. Quantum Chem. **25**, 347 (1984)
9. Nelander, B.: J. Chem. Phys. **51**, 469 (1969)
10. Srebrenik, S., Messer, R.: J. Chem. Phys. **63**, 2768 (1975)
11. Epstein, S. T.: The variation method in quantum chemistry, pp. 104–115. New York: Academic 1974
12. Takahata, Y., Parr, R. G.: Chem. Phys. Lett. **4**, 109 (1969)
13. Binkley, J. S., Whiteside, R. A., Krishnan, R., Seeger, R., DeFrees, D. J., Schlegel, H. B., Topiol, S., Kahn, L. R., Pople, J. A.: QCPE **13**, 406 (1981)
14. Walsh, A. D.: J. Chem. Soc. 2260 (1953)
15. Nakatsuji, H., Koga, T., in: The force concept in chemistry, pp. 137–217, Deb, B. M., ed. New York: Van Nostrand Reinhold 1981

Received November 8, 1983 / February 16, 1984